

# Laser Surface Modification of H13 Die Steel using Different Laser Spot Sizes

S.N.Aqida<sup>1,2</sup>, S.Naher<sup>1</sup>, and D.Brabazon<sup>1</sup>

<sup>1</sup>*School of Mechanical & Manufacturing Engineering, Dublin City University, Dublin 9, Ireland*

<sup>2</sup>*Fakulti Kejuruteraan Mekanikal, Universiti Malaysia Pahang, 26300 Kuantan, Pahang, Malaysia*

**Abstract.** This paper presents a laser surface modification process of AISI H13 tool steel using three sizes of laser spot with an aim to achieve reduced grain size and surface roughness. A Rofin DC-015 diffusion-cooled CO<sub>2</sub> slab laser was used to process AISI H13 tool steel samples. Samples of 10 mm diameter were sectioned to 100 mm length in order to process a predefined circumferential area. The parameters selected for examination were laser peak power, overlap percentage and pulse repetition frequency (PRF). Metallographic study and image analysis were done to measure the grain size and the modified surface roughness was measured using two-dimensional surface profilometer. From metallographic study, the smallest grain sizes measured by laser modified surface were between 0.51  $\mu\text{m}$  and 2.54  $\mu\text{m}$ . The minimum surface roughness,  $R_a$ , recorded was 3.0  $\mu\text{m}$ . This surface roughness of the modified die steel is similar to the surface quality of cast products. The grain size correlation with hardness followed the findings correlate with Hall-Petch relationship. The potential found for increase in surface hardness represents an important method to sustain tooling life.

**Keywords:** Laser spot size, grain size and surface roughness

## INTRODUCTION

The effect of surface roughness on component precision has been found to be strongly dependent on the laser beam energy [1]. The beam energy can be controlled by varying laser irradiance, number of pulses or pulse repetition frequency, and pulse duration. Increased laser irradiances have been seen to result in increased surface roughness [2]. High irradiance produces high pulse energy which can violently ablate the material's surface especially when processed at a slow scan rate. A reduced surface roughness ( $R_a$ ) of a thermal barrier coating by the laser glazing process was found with a reduction from 9  $\mu\text{m}$  to 4  $\mu\text{m}$  [3]. On the other hand, by increasing beam scanning speed and overlap, increased surface roughness can result in some cases [4, 5].

Increasing the number of pulses per step increases the interaction time which leads to higher laser energy absorption on the material's surface. When more laser energy was absorbed the surface temperature increases and forms irregular geometries which increase the surface roughness. The dependence of surface roughness on pulse width and pulse period was examined for laser processing of 316L steel (6). At 20 ms pulse period, the surface roughness was higher than measured for 80 ms pulse period processing. The pulse width ratio indicates the duty cycle setting during processing, where at 0.5 pulse width ratio the material-laser interaction time was only 50% of the fixed pulse period. At higher ratio, the surface roughness increased as the sample surface was more irradiated during the correspondingly longer interaction time.

In this study, the effect of laser beam spot size on the modified surface H13 die steel grain size and surface roughness was investigated. A low surface roughness of modified H13 die steel of 3  $\mu\text{m}$   $R_a$  or less is required in order to be used in many engineering applications especially the casting process.

## EXPERIMENTAL

The material investigated in this study was AISI H13 die steel with chemical composition given in **TABLE 1**. As-received 10 mm diameter H13 die steel cylindrical rods were sectioned into 120 mm length samples. The samples were cleaned with ethanol prior to processing. Samples were laser processed after surface roughening to produce  $3.0 \pm 0.2$   $\mu\text{m}$  average roughness and then chemically etched. A Rofin DC-015 diffusion-cooled CO<sub>2</sub> slab laser system with 10.6  $\mu\text{m}$  wavelength was used to modify the sample surface. The laser system was focused to a minimum laser spot diameter of 90  $\mu\text{m}$  onto the sample surface. To achieve larger laser surface beam spot diameters of 0.2 and 0.4 mm, the laser beam was also defocused from its focal position to a focal position above the surface. **TABLE 2** shows the parameter settings used to process the samples with three different spot sizes. The parameters

used were peak power,  $P_p$ , duty cycle, DC, overlap,  $\eta$ , and pulse repetition frequency, PRF. The outcome parameters from the settings were pulse duration,  $\tau$ , residence time,  $T_R$ , irradiance,  $I$ , and pulse energy,  $E_p$ .

Metallographic study was performed using an EVO-LS15, Carl Zeiss, scanning electron microscope (SEM) integrated with SmartSEM software. Samples were observed using back-scattered detector (BSD) at high vacuum. Grain size measurement was determined by Feret's diameter in Image J software (7-10). Two-dimensional surface profilometry was done using TR-200 measuring system integrated with TIME software to record the surface profile.

**TABLE 1.** Chemical composition of AISI H13 die steel

Material	Elements (wt%)										
	C	Mn	Si	Cr	Ni	Mo	V	Cu	P	S	Fe
H13	0.32-0.45	0.20-0.50	0.80-1.20	4.75-5.50	0.3	1.10-1.75	0.80-1.20	0.25	0.03	0.03	Bal.

**TABLE 2.** Samples processing parameters

Beam spot size (mm)	Sample	$P_p$ (W)	DC (%)	$\eta$ (%)	PRF (Hz)	Outcome parameters			
						$\tau$ (ms)	$T_R$ (ms)	$I$ (W/mm <sup>2</sup> )	$E_p$ (J)
0.4	E1	760	85	10	2857	0.298	0.32	5,548	0.23
	E2		100		2857	0.350	0.38		5,592
	E3		85	30	3810	0.223	0.29	4,618	0.17
	E4		100		3810	0.263	0.34	4,631	0.20
	E5		85		4000	0.213	0.32	3,971	0.16
	E6		100		4000	0.250	0.38	3,971	0.19
0.2	N1	507	49	50	2900	0.169	0.25	10,930	0.09
	N2	760	36			0.125	0.19	16,388	0.10
	N3	1313	23			0.080	0.12	28,184	0.11
0.09	F1	760	36	-10	2900	0.125	0.11	132,686	0.10
	F2	1515	18			0.062	0.06	264,499	
	F3	760	36	0	2300	0.157	0.16	119,297	0.12
	F4	1515	18			0.080	0.08	237,809	
	F5	760	36			0.125	0.14	108,582	
	F6	1515	18			0.062	0.07	216,449	

## RESULTS AND DISCUSSION

### Metallographic study

The laser irradiance as a function of residence time in laser surface modification of H13 die steels was plotted at three different spot sizes in **FIGURE 1**. At high laser irradiance of approximately 264 kW/mm<sup>2</sup> the residence time was 0.06 ms. At the lower laser irradiance of 3.9 kW/mm<sup>2</sup>, the residence time duration was set longer to 0.38 ms to melt the H13 steel surface. The effect of beam size on grain size of modified surface is shown by micrographs in **FIGURE 1**. Micrographs (a) to (d) in **FIGURE 1** depict the grain size observation at high magnification corresponding to the specific laser irradiance and residence time settings indicated. At 0.09 mm spot size processing, the laser irradiance ranged from 108 to 264 kW/mm<sup>2</sup> and residence times were between 0.06 ms and 0.16 ms. The irradiance range for 0.2 mm and 0.4 mm spot size processing was between 3.9 and 28 kW/mm<sup>2</sup> with a residence time range of 0.12 to 0.38 ms. Grain size of modified layer in micrograph (a), (b) and (c) of **FIGURE 1** was smaller compared to the as-received H13 die steel grain size in micrograph (d). The grain diameter linearly decreased with decreasing laser spot size used.

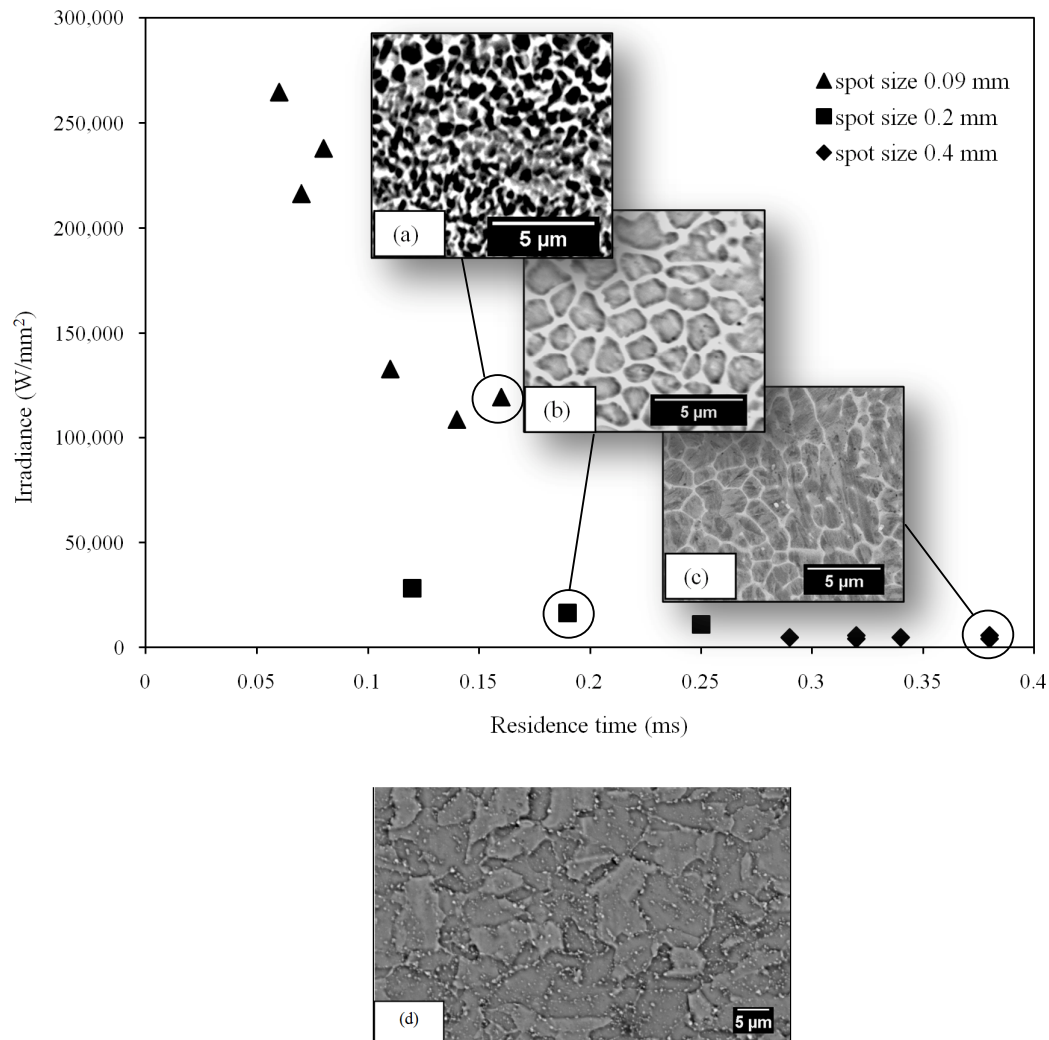


**FIGURE 1.** Micrographs of laser modified H13 samples processed at (a) 0.09, (b) 0.2 and (c) 0.4 mm spot size corresponding to the laser irradiance and residence time settings. As-received H13 die steel microstructure (d).

Decreasing spot size in processing H13 die steel influenced the sample surface morphology. The resulting surface morphology of the laser processed samples at different beam sizes is shown in the micrographs in **FIGURE 2**. The corresponding laser process conditions were of sample E5, N3 and F6. Micrographs (a) (c) and (e) in **FIGURE 2** show the surface of the sample processed at 0.4, 0.2 and 0.09 mm spot size respectively. **FIGURE 2** (b) shows varying molten pool depths of the sample processed with 0.4 mm spot size, where the maximum depth ranged from 135 to 205  $\mu\text{m}$ . Micrographs in **FIGURE 2** (d) and (f) depict consistent modified layer depths in the range of 70  $\mu\text{m}$  to 80  $\mu\text{m}$  produced by samples processed at 0.2 and 0.09 mm spot size. The molten pool geometrical pattern on the sample surface of **FIGURE 2** (a) was not consistent and not measurable in a similar manner to the other samples. The molten pool width measured from the sample processed at 0.2 mm spot size, **FIGURE 2** (c), was 245  $\mu\text{m}$ , while at 0.09 mm spot size, **FIGURE 2** (e), the width was 286  $\mu\text{m}$ . Bulging solidified molten pool geometries were observed in the micrographs of **FIGURE 2** (b) and (d) while a relatively flat surface was found for sample E5, shown in **FIGURE 2** (f).

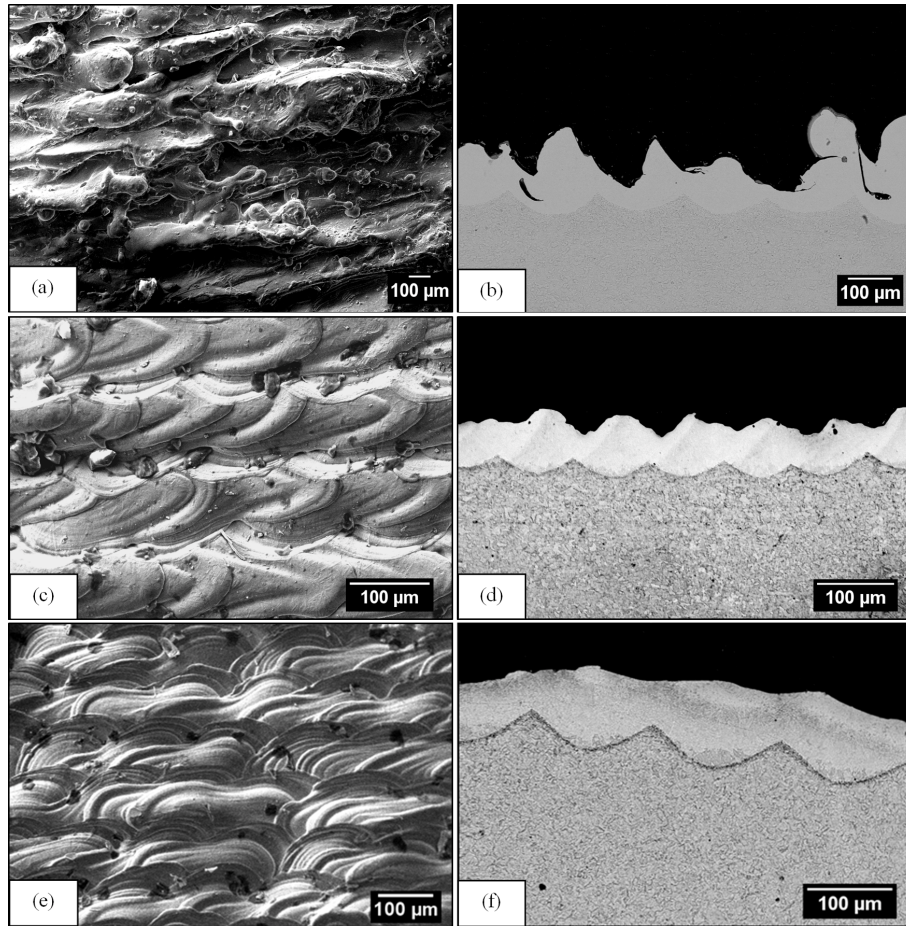


**FIGURE 2.** Molten pool width and thickness of samples processed at spot size 0.4 mm (a), (b) - [F6]; and 0.2 mm (c), (d) – [N3]; and 0.09 mm (e), (f) – [E5].

The range and distribution of grain sizes measured based on the Feret diameter, are given in **TABLE 3**. The Feret's diameter is the greatest straight line distance possible between any two points along the boundary of a region of interest (9, 10). The grain size of samples produced with the 0.4 mm spot size ranged from 2.54 to 5.99  $\mu\text{m}$  which was a large range when referred to the overall grain size distribution. At the smaller spot size of 0.2 mm and 0.09 mm, the range of grain sizes decreased.

Samples processed using 0.4 mm spot size produced a deeper modified surface due to higher duty cycle settings. The irradiance at 0.4 mm spot size was lower compared to the other spot sizes. Therefore, pulse duration was set between 0.20 and 0.35 ms regardless of the constant peak power.

At smaller spot sizes of 0.2 and 0.09 mm, the laser irradiance was higher due to the smaller affected area. The duty cycle was varied between 23 and 49% for different peak powers ranging between 507 and 1313 W when processed at 0.2 mm spot size. From the duty cycle setting, the resulting pulse duration range was 0.125 to 0.080 ms to limit the high irradiance interaction time with the surface. Samples processed using 0.09 mm spot size were set at peak powers of 760 and 1515 W and duty cycles of 18 and 36% to produce pulse durations ranging from 0.125 to 0.080 ms. Both spot sizes yielded similar ranges of average modified surface depth (between 70 and 80  $\mu\text{m}$ ) due to the similar range of pulse duration.

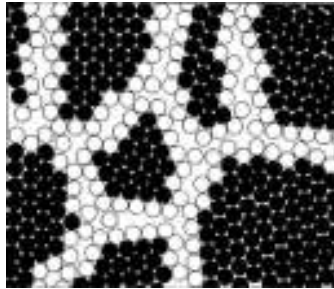
Low irradiance used with longer pulse duration roughened the modified surface due to softening before melting occurred. At higher laser irradiance the energy penetrates deep into the sample surface and forms definite solidified molten pools. The samples processed with spot sizes of 0.2 mm and 0.09 mm resulted in molten pool diameters which were multiples of the laser beam spot diameter due to the corresponding high irradiance levels.

**TABLE 3.** Range of modified H13 grain size processed at three laser spot sizes.

Laser spot size (mm)	Range of Feret diameter ( $\mu\text{m}$ )
0.40	2.54 – 5.99
0.20	1.60 – 2.83
0.09	0.51 – 1.09

Decreasing the laser spot size increased the heating and cooling rates. Change of heating and cooling rate was evidenced by the resulting observed different grain size ranges in the modified surface. Nano and ultrafine-grain size structures were developed in modified surface due to the large undercoolings produced from processing with a 0.09 mm spot size. **FIGURE 3** shows a schematic image of a nano-crystalline material where the grain-boundary atoms are white and are not clearly associated with crystalline symmetry [11]. The micrographs of samples processed at 0.2 mm and 0.09 mm spot size in **FIGURE 1** (a) and (b) clearly resemble the nano-crystalline structure. Nano-crystalline materials are characterized by a large volume fraction of grain boundaries and grain sizes have been observed to range between 10 and 300 nm [12]. The grain size range was found to vary greatly in this work with processing at a 0.4 mm spot size since the prolonged melting duration caused energy accumulation on the surface and recalescence. The local heat field and the local surface cooling rate can be varied greatly resulting in grain structure formation through the surface layers. The smaller spot size of 0.09 and 0.2 mm resulted in a more controlled surface temperature gradient due to short duty cycle. The ‘off’ state in laser pulse produced in these cases a sufficient time for development of undercooled austenite after each pulse and transformation to ultrafine-size ferrite ranging from 0 to 3  $\mu\text{m}$ . This is comparable with the austenite to ultrafine ferrite transformation obtained by thermo-mechanical controlled processing [13].

Consistent grain size distribution in the modified surface of samples processed with 0.09 and 0.20 mm spot size was possibly due to the large amount of grain boundary in the initial austenite phase. Similar trends have been previously recorded by other workers [14]. Initial austenite grain size was found from review to have a significant effect on the ferrite characteristics where the ferrite grain size distribution is more uniform for a fine initial austenite grain size when compared to an initial coarse austenite grain size [13]. On the other hand, at large undercoolings, the austenite grain size becomes less deterministic for final grain structure [15].

**FIGURE 3.** 2D model of a nano-structured material. The atoms in the centres of the crystals are indicated in black (11).

## Surface Roughness

Surface roughness results varied with pulse energy and laser spot size as given in **TABLE 4**. The average surface roughness ( $R_a$ ) achieved in samples processed with 0.4 mm spot size ranged between 5.1 and 36.1  $\mu\text{m}$  with the two significant determining factors identified as overlap and duty cycle, which are in agreement with previous work [6, 16]. The minimum surface roughness was achieved in samples processed at the minimum overlap of 10% and at a duty cycle of 85%. Increasing both the number of pulses and the duty cycle increased the material-laser interaction time which leads to higher laser energy absorption [4, 5]. When more laser energy was absorbed the surface temperature increased and formed irregular geometries which increased the surface roughness [1, 17].

**TABLE 4.** Surface roughness of laser modified H13 tool steel processed at three different spot sizes.

Spot size (mm)	0.09						0.2				0.4				
	F1	F2	F3	F4	F5	F6	N1	N2	N3	E1	E2	E3	E4	E5	E6
$R_a$ ( $\mu\text{m}$ )	6.1	3.0	22.4	5.0	5.5	3.9	3.1	7.9	6.2	5.1	31.4	11.0	31.7	22.8	36.1

A lower range of surface roughness was recorded in samples processed with 0.2 mm spot size compared to samples produced at 0.4 mm spot size. Although high irradiance settings, a 0.2 mm spot size might be expected to cause an increase of surface roughness, the pulse energies and durations were reduced compared to samples processed at 0.09 mm spot size [2, 17, 18]. Among the three samples processed using 0.2 mm spot size, the surface roughness was lower in sample N1 where the pulse energy was lowest at 0.09 J. Higher surface temperature which resulted from a higher irradiance, improved the surface absorptance which promoted energy penetration and efficient surface melting. The surface temperature was lower for small pulse energy processing and improved surface topography resulted.

Higher laser irradiance was designed into sample processing conditions for the 0.09 mm spot size, with two levels of peak power. A higher range of surface roughness was measured for these samples, between 3.0 and 22.4  $\mu\text{m}$ , in comparison to measurements taken from samples processed with a 0.2 mm spot size. Increase of surface roughness for sample N2 was contributed to by the high duty cycle setting at the low peak power of 760 W. While duty cycle determines the pulse duration, an increase of overlapped pulses prolongs the laser-surface interaction time, both of which affect the surface temperature. However, decreasing the duty cycle at the high power setting can minimise the surface roughness at any overlap setting due to the dominance of duty cycle effect at the higher power setting.

## CONCLUSIONS

Variation of spot size in laser surface modification process affects the outcome parameters such as irradiance and residence time. Using the smaller spot size of 0.09 mm, a higher irradiance and a shorter residence time were produced, while the larger spot sizes of 0.2 and 0.4 mm decreased irradiance and necessitated longer residence times in order to melt the H13 die steel surface. The smaller spot size of 0.09 mm resulted in modified samples with ultrafine grain size which is provide for high hardness properties. Processing at the higher irradiance level with lower duty cycle resulted in lower surface roughness. These findings are useful for designing materials surface modification regimes using the CO<sub>2</sub> laser system as grain size and surface roughness properties are crucial requirements in the many engineering applications for this material.

## ACKNOWLEDGMENTS

The authors would like to thank Dublin City University and the Ministry of Higher Education Malaysia for funding the research.

## REFERENCES

1. L. M. Cabalín, D. Romero, J. M. Baena and J. J. Laserna, *Surf. Interface Anal.* **27**, 805-810 (1999).
2. T. Li, Q. Lou, J. Dong, Y. Wei and J. Liu, *Appl. Surf. Sci.* **172**, 331-344 (2001).
3. P. Tsai, J. Lee and C. Chang, *Surf. Coat. Technol.* **202**, 719-724 (2007).
4. W. Jiang and P. Molian, *Surf. Coat. Technol.* **135**, 139-149 (2001).
5. C. Batista, A. Portinha, R. M. Ribeiro, V. Teixeira, M. F. Costa and C. R. Oliveira, *Appl. Surf. Sci.* **247**, 313-319 (2005).
6. A. J. Pinkerton and L. Li, *Appl. Surf. Sci.* **208-209**, 411-416 (2003).
7. K. S. Raju, M. G. Krishna, K. A. Padmanabhan, K. Muraleedharan, N. P. Gurao and G. Wilde, *Mater. Sci. Eng., A* **491**, 1-7 (2008).
8. P. J. Lee, R. Ruess and D. C. Larbalestier, *IEEE Trans. Appl. Supercond.* 1516-1519 (1997).
9. W. H. Walton, *Nat.* **162**, 329-330 (1948).
10. S. Al-Thyabat and N. J. Miles, *Powder Technol.* **166**, 152-160 (2006).
11. H. Gleiter, *Acta Mater.* **48**, 1 (2000).
12. M. A. Meyers, A. Mishra and D. J. Benson, *Prog. Mater. Sci.* **51**, 427-556 (2006).
13. Y. Adachi, M. Wakita, H. Beladi and P. D. Hodgson, *Acta Mater.* **55**, 4925-4934 (2007).
14. S. C. Hong and K. S. Lee, *Mater. Sci. Eng., A* **323**, 148-159 (2002).
15. T. Yokota, C. García Mateo and H. K. D. H. Bhadeshia, *Scr. Mater.* **51**, 767-770 (2004).
16. H. J. Shin and Y. T. Yoo, *J. Mater. Process. Technol.* **201**, 342-347 (2008).
17. C. N. Panagopoulos, A. E. Markaki and P. E. Agathocleous, *Mater. Sci. Eng., A* **241**, 226-232 (1998).
18. A. J. Pinkerton and L. Li, *Appl. Surf. Sci.* **208-209**, 405-410 (2003).